Yolk-shelled MoS_2/C@Void@C@MoS_2 nanospheres as stable and high-rate anode in sodium/potassium ion batteries

Mang Niu*[a], Zongfan Zhu[b], Zhenkai Mou[b], Wenpei Kang*[b]

a State Key Laboratory of Bio-fibers and Eco-textiles, Institute of Biochemical Engineering College of Materials Science and Engineering, Qingdao University, Qingdao 266071, P. R. China. E-mail: mang.niu@qdu.edu.cn

b School of Materials Science and Engineering, China University of Petroleum (East China), Qingdao, 266580, P. R. China. E-mail: wpkang@upc.edu.cn

Experimental Section

Preparation of yolk-shelled MoS_2/C@Void@C@MoS_2 nanosphere

The polypyrrole-phosphomolybdic acid (PPy-PMo_{12}) nanospheres was first synthesized according to our previous work. Then the obtained PPy-PMo_{12} powder was dispersed into a mixed solution containing of 70 mL ethanol, 10 mL deionized water and 3.0 mL ammonia under the ultrasonication for 10 min. Then the tetrapropoxysilane (0.5 mL) was added into the above suspension under the stirring, followed by the addition of resorcinol (0.1 g) and formaldehyde (0.1 mL) and stirring for 24 h. After that, the precipitate was collected via repeated washing with deionized water and ethanol by centrifugation, resulting into SiO_2 and resorcinol-formaldehyde (RF) double-layer coated PPy-PMo_{12} spheres (PPy-PMo_{12}@SiO_2@RF).

The obtained dried PPy-PMo_{12}@SiO_2@RF powder was heated to 700 ℃ with the heating rate of 2 ℃ min^{-1} and kept for 2 h in the Ar atmosphere. After cooling down to room temperature, the product was etched in 10% HF solution for 12 h to remove the SiO_2 coating layer. Then the obtained powder (50 mg) was dispersed into deionized water (40 mL), followed by the addition of sodium molybdate dehydrate (20 mg) and l-cysteine (50 mg) under stirring for 30 min. The above solution was sealed in a Teflon-lined stainless steel autoclave and reacted at 200 ºC for 12 h. After cooling down, the precipitate was collected through centrifugation and washed with deionized water and ethanol for three times. The sample was dried at 60 ℃, producing MoS_2 and carbon layer coated carbon coupled MoS_2 (MoS_2/C) nanospheres with yolk shelled structure (MoS_2/C@Void@C@MoS_2). In addition, using the similar procedure except for the absence of sodium molybdate dehydrate during the sulfidation process, MoS_2/C

nanosphere was prepared with the PPy-PMo_{12} precursor, while the yolk shelled carbon coated MoS_2/C (MoS_2/C@Void@C) was also obtained with the PPy-PMo_{12}@SiO_2@RF precursor.

Characterization of Materials

The structure properties of the samples were conducted on field-emission scanning electron microscope (FESEM; JSM-7200F) and transmission electron microscope (TEM; JEOL, JEM-2100). The phases was analysed on Bruker a AXS D8 Advance with Cu Kα (λ = 1.5418 Å, 40.0 kV, 30.0 mA). The oxidation states of the elements in the samples were collected from X-ray photoelectron spectrometer (XPS, Thermo ESCALAB 250). Raman spectra were obtained on HORIBA Evolution Raman scope using excitation laser of 532 nm.

Electrochemical Measurements

In order to evaluate the electrochemical performance in the SIBs and PIBs, the obtained MoS_2/C@Void@C@MoS_2, MoS_2/C@Void@C, and MoS_2/C were first prepared into working electrodes. The active materials, carbon black and sodium carboxymethyl cellulose (CMC) binder with the weight ratio of 6: 2: 2 were fully grounded and mixed in the water to form a homogenous slurry. Then it was pasted on the copper foils and dried overnight at 80 °C, which were cut into working electrodes with diameters of 12 mm. The coin cells were assembled using sodium or potassium slices as counter electrodes in a glove box with Ar atmosphere (H_2O <0.01 ppm, O_2 <0.01 ppm). The electrolyte of the SIBs is $NaClO_4$ solution (1.0 mol L^{-1}) in propylene carbonate (PC) with 10% fluoroethylene carbonate (FEC), while $K[(FSO_2)_2N]$ (KFSI) solution (1.0 mol L^{-1}) in ethylene carbonate/diethyl carbonate (EC/DEC v/v = 1:1) was selected for PIBs. The separators used in the SIBs/PIBs are Whatman GF/D glass fiber membranes. On the Neware-5 V10/20 mA battery system (Shenzhen Xinwei), the galvanostatic charge/discharge cycling and the galvanostatic intermittent titration technique (GITT) were conducted. As for the GITT, the cells were charged/discharged at 0.05 A g^{-1} for 24 min, and a following resting for 12 min, in order to determine sodium-ion diffusion coefficient (D_{Na}) and potassium-ion diffusion coefficient (D_K). The electrochemical impedance spectroscopy (EIS) (0.1 Hz ~ 100 kHz for SIBs; 0.01 Hz ~ 100 kHz for PIBs) and cyclic voltammetry (CV) curves with sweep rates from 0.1 to 1.0 mV s^{-1} were measured on the Gamary 30115 electrochemical workstation.

Density functional theory (DFT) calculations

The DFT calculations were carried out using the Vienna Ab-initio Simulation Package

(VASP)[1,2] with the frozen-core all-electron projector-augment-wave (PAW)[3,4] method. The Perdew-Burke-Ernzerhof (PBE)[5] of generalized gradient approximation (GGA) was adopted to describe the exchange and correlation potential. The cutoff energy for the plane-wave basis set was set to 450 eV. A 2-layer 5×5 carbon supercell was used, and a vacuum region of 20 Å above them were used to ensure the decoupling between neighboring systems. A mono-layer 4×4 MoS_2(001) slab was placed below the 5×5 carbon slab to build the model of C@MoS_2 composite. The geometry optimizations were performed until the forces on each ion was reduced below 0.01 eV/Å, and a 3×3×1 Monkhorst-Pack k-point[6] sampling of the Brillouin zone was used. The van der Waals (vdW) interactions have been considered by using DFT-D3 method of Grimme[7]. The climbing image nudged elastic band (CI-NEB)[8,9] method was adopted to calculate the diffusion path and energy barrier of Na^+ and K^+ in carbon and carbon@MoS_2 composite.

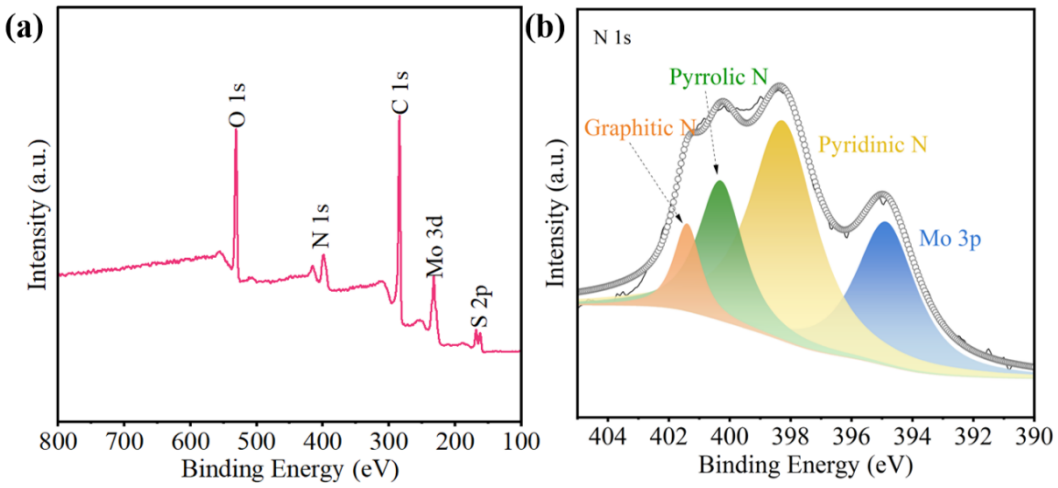

Fig. S1. (a) The survey and (b) the high-resolution N 1s spectra of the MoS_2/C@Void@C@MoS_2 nanosphere.

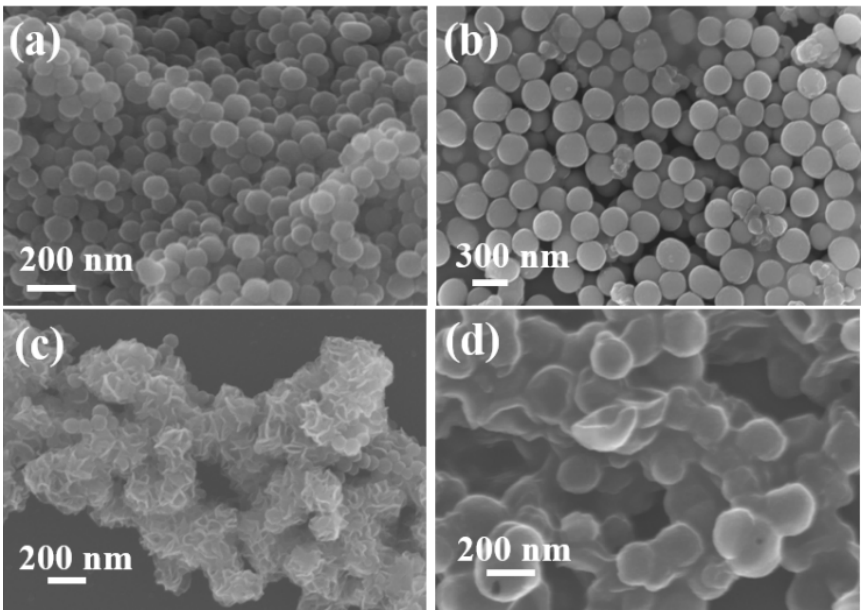

Fig. S2. SEM images of (a) PPy-PMo_{12}, (b) PPy-PMo_{12}@SiO_2@RF, (c) MoS_2/C and (d) MoS_2/C@Void@C.

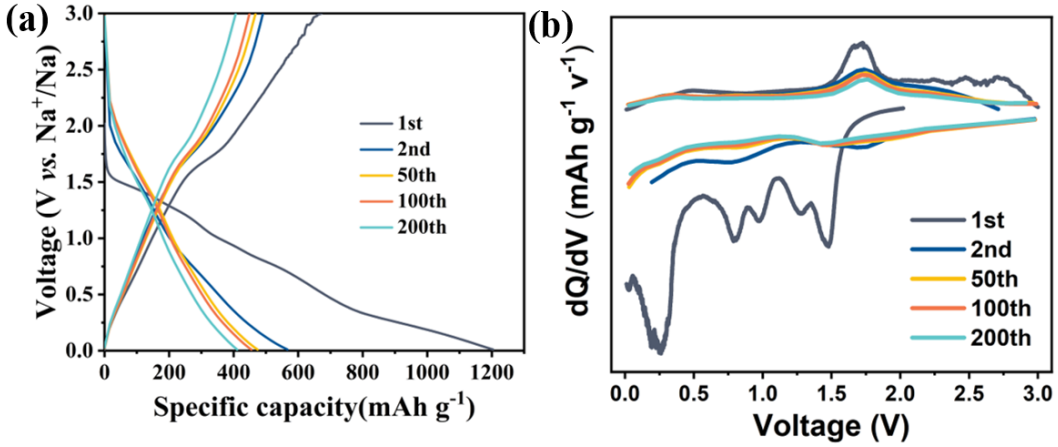

Fig. S3. (a) The selected discharge/charged profiles and (b) the related dQ/dV curves of MoS_2/C@Void@C@MoS_2 anode at 1.0 A g^{-1} after the low current activation with 50 mA g^{-1} in SIBs.

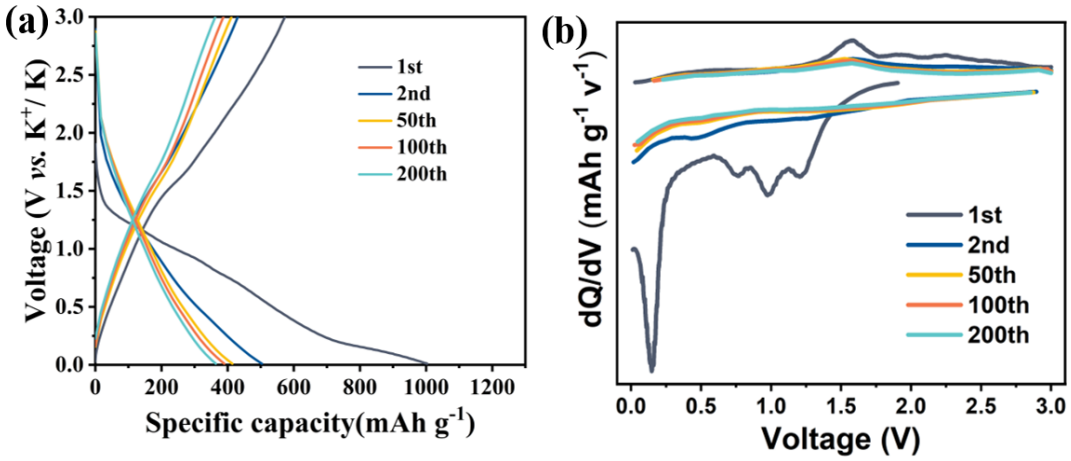

Fig. S4. (a) The selected discharge/charged profiles and (b) the related dQ/dV curves of MoS_2/C@Void@C@MoS_2 anode at 1.0 A g^{-1} after the low current activation with 50 mA g^{-1} in PIBs.

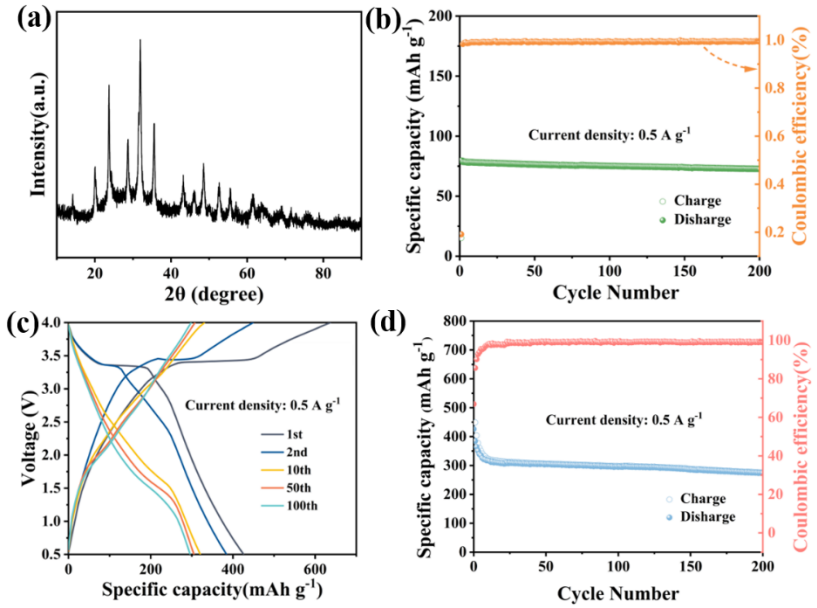

Fig. **S5.** (a) The XRD patterns and (b) cycling performance at 0.5 A g^{-1} of the home-made $Na_3V_2(PO_4)_3$@C[10]; (c) The selected charge-discharge profiles and (d) the cycling performance of the MoS_2/C@Void@C@MoS_2//$Na_3V_2(PO_4)_3$@C full cell at 0.5 A g^{-1}.

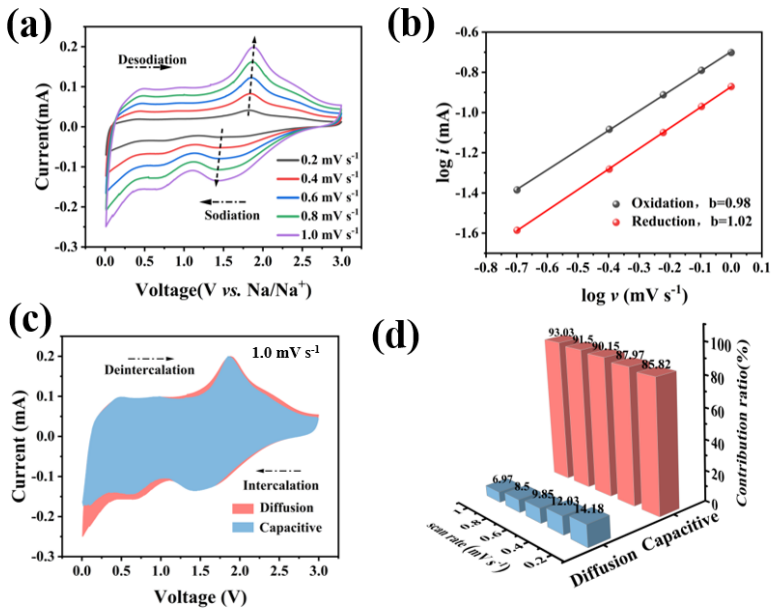

Fig. S6. (a) CV curves with different scan rates, (b) the peak current against scan rates, (c) The separation of capacity contribution at the scan rate of 1.0 mV s^{-1} and (d) the capacitive contribution ratios at different scan rate for the MoS_2/C@Void@C@MoS_2 anode in SIBs.

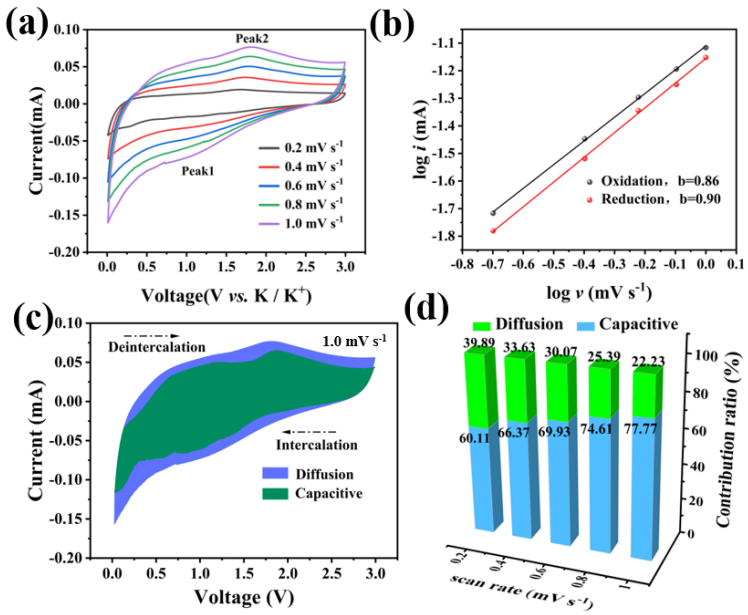

Fig. S7. (a) CV curves with different scan rates, (b) the peak current against scan rates, (c) the separation of capacity contribution at the scan rate of 1.0 mV s^{-1} and (d) the percentage of capacitive contributions at different scan rate for the MoS_2/C@Void@C@MoS_2 anode in PIBs.

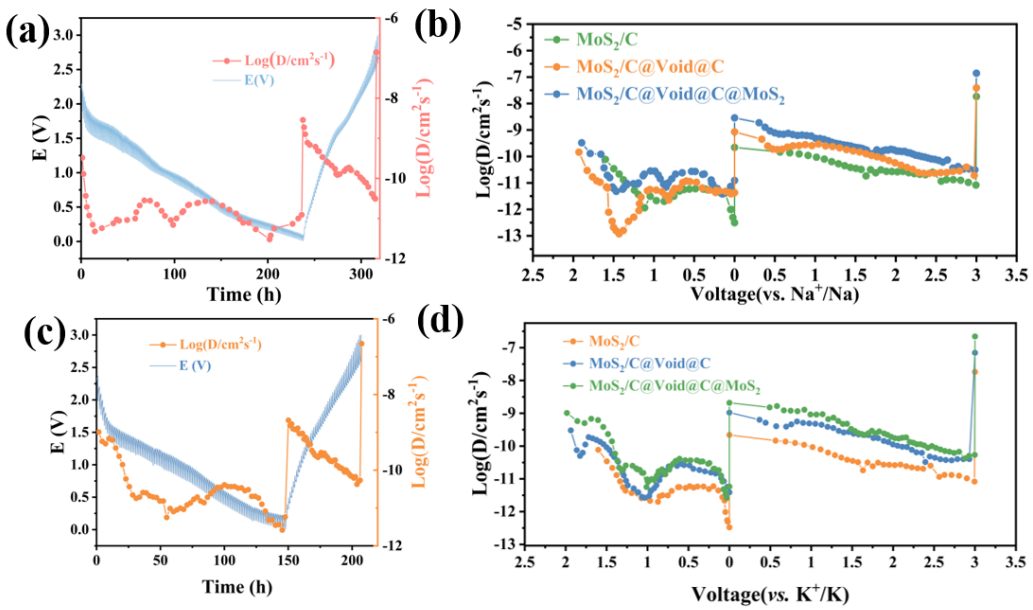

Fig. S8. (a) GITT curves and their related D_{Na} values for MoS_2/C@Void@C@MoS_2 anode and (b) D_{Na} value comparison at different discharge/charge states of the three samples in SIBs; (c) GITT curves and their related D_K values for MoS_2/C@Void@C@MoS_2 and (d) D_K value comparison at different discharge/charge states of the three samples in PIBs.

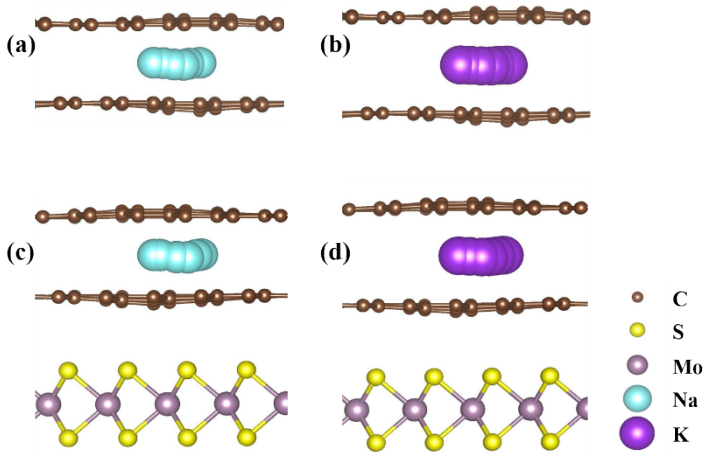

Fig. S9. The optimized Na^+ diffusion path in (a) carbon and (c) carbon@MoS_2; The optimized K^+ diffusion path in (b) carbon and (d) carbon@MoS_2.

References

1. G. Kresse, and J. Hafner, *Phys. Rev. B*, 1994, **49**, 14251-14269.

2. G. Kresse and J. Furthmüller, *Phys. Rev. B*, 1996, **54**, 11169-11186.

3. P. E. Blöchl, Phys. Rev. B, 1994, **50**, 17953-17979.

4. G. Kresse and D. Joubert, *Phys. Rev. B*, 1999, **59**, 1758-1775.

5. B. Hammer and L. B. Hansen, *Phys. Rev. B*, 1999, **59**, 7413-7421.

6. H. J. Monkhorst, J. D. Pack, *Phys. Rev. B*, 1976, **13**, 5188-5192.

7. S. Grimme, *J. Comput. Chem.*, 2006, **27**, 1787–1799.

8. G. Henkelman and H. Jónsson, *J. Chem Phys.*, 2000, **113**, 9978.

9. D. Sheppard, R. Terrell and G. Henkelman, *J. Chem Phys.*, 2008, **128**, 134106.

10. W. Duan, Z. Zhu, H. Li, Z. Hu, K. Zhang, F. Cheng and J. Chen, *J. Mater. Chem. A*, 2014, **2**, 8668-8675.